IOPscience iopscience.iop.org

Home Search Collections Journals About Contact us My IOPscience

Theoretical simulation of free carrier mobility collapse in GaN in terms of dislocation walls

This article has been downloaded from IOPscience. Please scroll down to see the full text article.

2000 J. Phys.: Condens. Matter 12 10213

(http://iopscience.iop.org/0953-8984/12/49/321)

View the table of contents for this issue, or go to the journal homepage for more

Download details:
IP Address: 171.66.16.226
The article was downloaded on 16/05/2010 at 08:10

Please note that terms and conditions apply.

J. Phys.: Condens. Matter **12** (2000) 10213–10221. Printed in the UK PII: S0953-8984(00)17836-1

Theoretical simulation of free carrier mobility collapse in GaN in terms of dislocation walls

J-L Farvacque†, Z Bougrioua‡ and I Moerman‡

† LSPES, Université des Sciences et Technologies de Lille, 59650 Villeneuve d'Ascq, France
‡ INTEC, IMEC—Ghent University, Sint-Pietersnieuwstraat 41, 9000 Ghent, Belgium

Received 9 October 2000

Abstract. Using low field electrical transport simulations, we show that the particular mobility behaviour versus carrier density in MOVPE GaN materials, characterized by a mobility collapse at low dopant densities, cannot be simply interpreted in terms of dislocation scattering or trapping mechanisms, but that it is also controlled by the collective effect of dislocation walls (the columnar structure). As the free carrier density increases, the more efficient screening properties result in the transition between a barrier-controlled mobility regime and a pure-diffusion-process-controlled mobility regime. The model permits us to quantitatively reproduce the experimental mobility collapse.

1. Introduction

The free carrier mobility versus carrier density in n-type GaN grown by low-pressure metallorganic vapour phase epitaxy (LP-MOVPE) on sapphire substrates has often been found extremely low at low n-type doping level while it reaches standard values for larger doping. This behaviour is singular when compared to the classical behaviour that shows that the carrier mobility is mainly controlled by ionized impurity scattering and as a consequence the lower the doping level the larger the carrier mobility [1–4]. In our experiments, the mobility versus carrier density presents an even clearer trend as it displays a sharp transition which separates a low mobility regime, as long as the carrier density is lower than a critical value, from a large mobility regime (the so-called mobility collapse in [5] and [6]). This behaviour has been met for several series of samples grown by LP-MOVPE using the two step procedure described in [7]. Figure 1 shows an example of two sets of experimental points corresponding to two families of layers grown with two different growth processes: the transitions occur at about 8×10^{17} cm^{-3} and 2×10^{17} cm^{-3} respectively for series α and series Ω. For each series, the only variable parameter is the concentration of the Si dopant (diluted silane). Samples belonging to a given series are then expected to possess quite identical defect substructures and should mainly differ from their doping densities. Our experimental procedure allows us to eliminate the result dispersion in results found in literature. TEM observations [5, 8] indicate that any of our samples is, as usual, characterized by a columnar cell structure constituted by threading dislocations more or less arranged in walls (rough sub-grain boundaries). A rough estimate of the dislocation density is about 2×10^{10} and 5×10^{9} cm^{-3} for respectively series α and series Ω.

Classical transport approaches [5, 6, 9–13] remain quite unable to describe the sharp collapse of the mobility versus the free carrier density for a given temperature. In [5] and [6],

0953-8984/00/4910213+09$30.00 © 2000 IOP Publishing Ltd

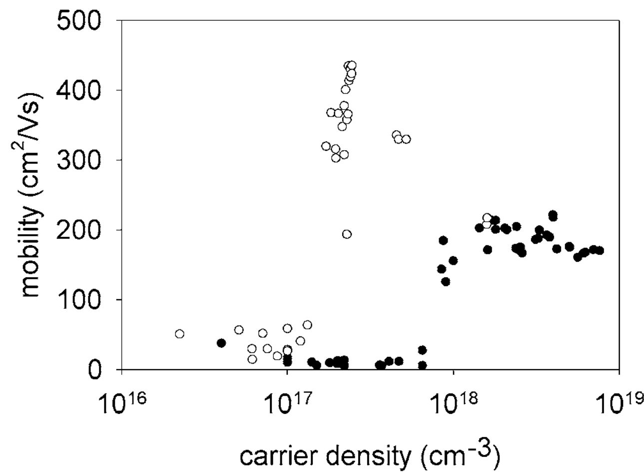

Figure 1. Evolution of the 300 K Hall carrier mobility as a function of the Hall carrier density for two sets of GaN layers: series α (black circles) and series Ω (white circles), each grown with a specific growth process [8].

we have already reported that this behaviour cannot be described by assuming that dislocations only act as scattering centres. In the present article, we qualitatively and quantitatively show that it results from the presence of dislocation walls (i.e. the dislocation substructure) which act as electronic barriers as long as the screening properties of the material remain quite unable to separate the energy band bending arising from neighbouring dislocations of a given wall.

2. Transport analysis in terms of diffusion process

2.1. The theoretical framework of the present simulation

In the particular case of GaN which contains a very large dislocation density and which is also characterized by a very large energy of the optical phonons (91 meV), we expect that the carrier mobility will strongly depend on (i) the concentration of dislocations, which are the typical examples of *anisotropic* scattering centres, as well as on (ii) optical phonon scattering mechanisms, which are the prototype of *inelastic* scattering mechanisms. Thus, we have grounded the present simulation in the frame of the so-called *dynamical transport theory*. This recent approach allows us to deal, in a consistent manner, with anisotropic [14] as well as with inelastic [15] scattering mechanisms contrarily to the classical relaxation time approximation (although it is generally used in the referred literature), which cannot be extended, in principle, to such scattering mechanisms [16].

2.2. Dislocation states

Ab initio calculations unambiguously indicate that, for GaN [17], the dislocation core structures are arranged in such a way that only shallow one-dimensional densities of states are present below the conduction band or above the valence bands. A precise numerical calculation of such shallow states was undertaken in [18], in the framework of the envelope function approximation, by assuming that they originate from long range binding potentials connected with the dislocation strain field through the deformation potential and piezoelectric potential coupling. In this approach, the ‘a-edge’ threading dislocations in GaN (those which are mainly

involved in the formation of sub-grain boundaries of the columnar cell structure) should bind shallow electronic states lying at about 100 meV under the conduction band. Nevertheless, because of their Cottrell atmosphere (made up of segregated impurities or point defects), as-grown dislocations may also bind localized states through extrinsic mechanisms rather than because of the intrinsic properties recalled above. Thus, the existence and location of dislocation energy states remain open questions and we consider, in the following, such states and their location E_{dislo} under the conduction band as being a free parameter for fitting our mobility measurements.

Dislocation states are closely spaced all along the dislocation line. Thus, it is clear that carriers trapped on such states interact electrostatically, increasing therefore the free energy of the whole system. This results in a self-regulation of the dislocation state statistics which has been described in various models, for instance the depleted region around the dislocation line [19] (similarly to what is done for the study of Schottky diodes), or again the Debye–Hückel screening [20]. Such dislocation statistics have also been included in our simulation.

2.3. Dislocation scattering mechanisms

Concerning dislocations, the study of their role on the mobility of GaN is surprisingly restricted in the referred literature [9, 10, 12, 13] to the so-called 'core effect' scattering mechanisms (issuing from the linear charge trapped at the dislocation line) though it has been known for a long time that the dislocation strain field also prompts other scattering mechanisms through the deformation potential and the piezoelectric coupling [21]. Such dislocation scattering mechanisms have been included in the present simulation. In the particular case of GaN, the piezoelectric tensor is such that dislocations parallel to the c axis (in practice the threading dislocations) do not couple into any piezoelectric potential [22]. However, we nonetheless introduced in our simulation the possibility that a given fraction of dislocations could have 'non-vertical' orientations (with the c axis being the 'vertical') and induce some piezoelectric scattering potentials

2.4. Theoretical results in terms of pure diffusion mechanism

Simulation of the mobility in terms of pure diffusion processes have been undertaken, including all the contributions recalled in the above sub-sections and considering as other scattering mechanisms the ionized impurities, acoustical and optical phonons and carrier–carrier scattering. The physical parameters used are the standard values found in literature. Figure 2 shows a typical determination of the mobility versus carrier density, at room temperature, for various dislocation densities and a compensation ratio arbitrarily chosen equal to 0.3. It more particularly shows that dislocations mainly act as efficient scattering centres at low carrier density while their scattering effect is less and less preeminent in the heavily doped range. In any case, it is impossible to obtain mobilities as low as those measured experimentally in the low mobility range without introducing unrealistic dislocation densities. Whatever the density of dislocations and the position of their bound states, we are unable to reproduce the singular behaviour shown in figure 1.

3. A dislocation barrier model

The idea of a barrier controlled mobility has already been suggested for polycrystalline silicon films [23], further extended to GaN in [24] and used in [25] to explain the thermally activated conductivity in undoped GaN layers. However, this kind of model is unable to explain the

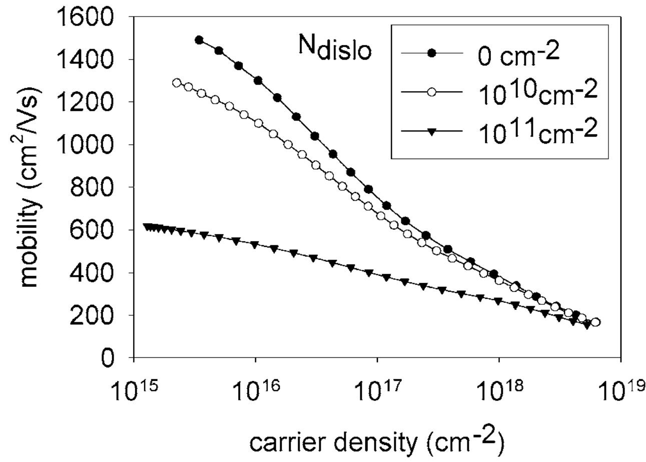

Figure 2. Mobility versus carrier density at 300 K for various dislocation densities. In all the cases, the compensation ratio $C = N_A/N_D$ is 0.3.

sharp mobility transition or again the existence of a critical carrier density at which it occurs. In our former approach in [6], the internal barriers associated with the walls of dislocations were supposed to have fixed height and were overcome by the carriers, because of a subsequent motion of the Fermi level when increasing the dopant density. Typically, such a model leads to a fixed critical density at which the sharp mobility transition occurs and which roughly corresponds to the transition between the non-degenerate and the degenerate electron gas behaviour, when increasing the dopant density (i.e. at a value lying near the intrinsic conduction band density of states at about $\sim 2 \times 10^{18}$ cm^{-3}). Thus, it was impossible to explain why this critical carrier density value would depend on the defect substructure and could be as low as 2×10^{17} cm^{-3} as obtained in the second series of GaN layers (series Ω) presented in figure 1.

In the present model, we suppose that dislocations are responsible for localized energy states closely spaced all along their line. Because of a large density of states, such levels are attracted, at equilibrium, by the Fermi level and, in the rigid shift approximation, a resulting band bending occurs around the dislocation line, in a similar way to what happens in the depleted region of a Schottky diode. Figures 3(a) and (b) illustrate such a band bending.

The band bending shape $E_C(r)$ may be found by assuming that, within a given radius R, the area surrounding the dislocation line is depleted. Then, using the boundary conditions $E_C(0) = E_F - E_{dislo}$ and $E_C(R) = 0$, Poisson's equation integration gives

$$E_C(r) = (E_F - E_C) - \frac{K_B T}{4} \frac{r^2}{\lambda^{*2}} \text{ for } r < R \qquad \text{else } E_C(r) = 0 \tag{3.1}$$

$$R = 2\lambda^* \sqrt{\frac{E_F - E_{dislo}}{K_B T}} \tag{3.2}$$

where we have introduced the screening wavelength given by $\lambda^{*2} = \varepsilon_0 \varepsilon_L K_B T/(N_D^+ - N_A^-)e^2$.

We consider now a family of neighbouring dislocations belonging to a sub-grain boundary (one dislocation wall). Such dislocations should result in the existence of an internal electronic barrier as long as the mean distance d separating two neighbouring dislocations is smaller than $2R$ (figure 3(d)), otherwise dislocations may be considered as independent scattering centres (figure 3(c)). Thus, a criterion which separates the barrier-controlled mobility from a pure

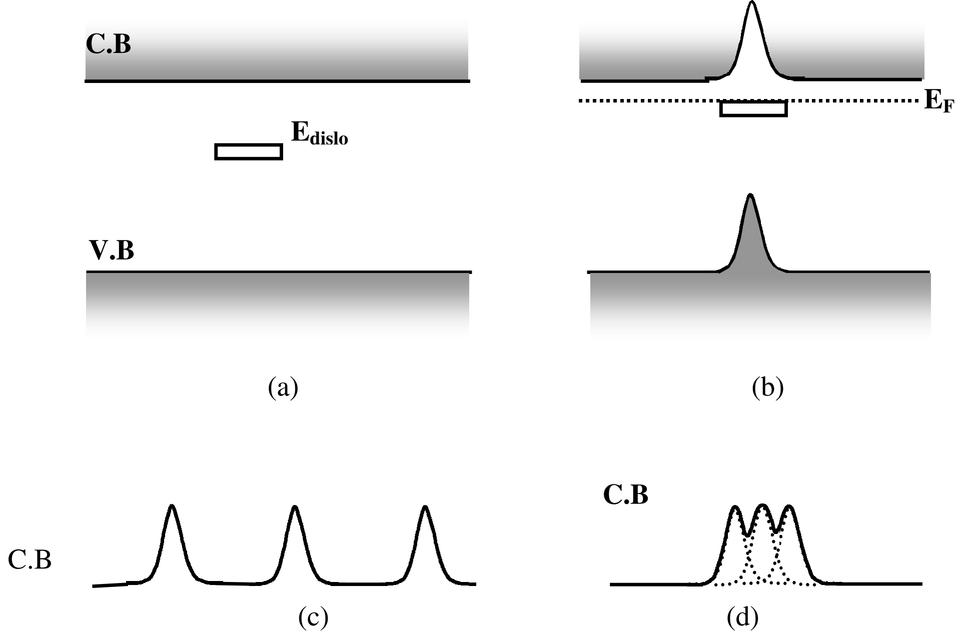

Figure 3. Schematic representation of the dislocation induced band bending of the conduction band. (a) A neutral dislocation; (b) represents a charged dislocation of which the energy level is shifted towards the Fermi energy level. (c) Individual dislocations. (d) A barrier induced by dislocations.

diffusion process is

$$d < 4\lambda^* \sqrt{\frac{E_F - E_{dislo}}{K_B T}} \rightarrow \text{barrier controlled mobility.} \tag{3.3}$$

When $d < 2R$, the energy at the saddle point E_{spt} of the barrier, localized between two neighbouring dislocations, is given by

$$E_{spt}(r) = 2\left((E_F - E_{dislo}) - \frac{K_B T}{16}\frac{d^2}{\lambda^{*2}}\right) \tag{3.4}$$

while its thickness d_{spt} is approximately given by

$$d_{spt} = 2\sqrt{R^2 - \frac{d^2}{4}}. \tag{3.5}$$

So let us now approximate the barrier saddle point to a square potential barrier of energy height E_{spt} and thickness d_{spt}. We attribute to this point a tunnel transmission power $T(\varepsilon)$ for which the expression can be found in any textbook. In a barrier-free material, each carrier of energy $\varepsilon(k)$ statistically contributes to the final conductivity through the elemental contribution to the current density $j_k = e\delta f_k v_k$ where $v_k = \hbar k/m^*$ is the carrier velocity. δf_k is the modification brought to the Fermi–Dirac occupation function of state k by the applied external field F_{appl}. As soon as such a carrier meets a potential barrier, it contributes in fact to the whole current by the effective elemental contribution $j_k^* = T(\varepsilon_k) j_k$. Thus, the whole current density in the presence of barriers is given by

$$j^* = 2e \int T(\varepsilon_k)\delta f_k v_k n_k \, \mathrm{d}^3 k \tag{3.6}$$

where n_k is the k density of states.

4. Donor statistics

Our model strongly depends on the location of the Fermi energy E_F, which is determined by solving the neutrality equation. Thus, it is strongly dependent on the description of the donor statistics. It is, however, clear that the experimental results shown in figure 1 range from a region where the material is 'moderately' doped towards a region where it is 'heavily' doped. This introduces some particular features in the donor statistics.

(a) The free carrier screening modifies the position of the donor binding energy E_D. This point has been overcome by looking for the minimum versus r of the following equation:

$$E_D = \frac{p^2}{2m^*} - \frac{e^{-r/\lambda_{DH}}}{4\pi\varepsilon_0\varepsilon_L r} \tag{4.1}$$

when the Heisenberg relation $pr = \hbar$ is considered and where λ_{DH} is the Debyg–Hückel screening wavelength. Note that the formula $pr = \hbar$ corresponds in fact to the application for the ground state of the Heisenberg relation $\Delta p\ \Delta r = \hbar$. The minimum of (4.1) leads to the classical hydrogenic model when the wavelength is infinite while it leads to figure 4 in the presence of a free carrier density n. It clearly indicates that the donor binding energy $E_D(n)$ vanishes for n values larger than $\sim 1.5 \times 10^{18}$ cm^{-3} for $m^* = 0.22\, m_0$ and $e_L = 8.9$. Above these values all the donors must be considered as ionized.

(b) Increasing the donor density also results in the appearance (i) of an impurity band as soon as the bound state radius $r = a^*$ (at which (4.1) is minimum) becomes comparable to the mean spacing d between impurities and (ii) of some conduction band tailing. To include such effects,

(i) We have phenomenologically introduced the following donor density of states:

$$N_D(E) = N_D \frac{1}{\sigma\sqrt{\pi}}\, \mathrm{e}^{-((E-E_D)/\sigma)^2} \tag{4.2}$$

where N_D is the donor density and where σ is a parameter representing typically the dispersion in the interaction energy between a bound carrier and its neighbours because of their random distribution. It is clear that for low doping, the mean impurity spacing is large, leading to negligible interactions and therefore to small sigma values. In such cases, the Gaussian function acts as a Dirac function of width σ so that

$$\lim_{\sigma\to 0} N_D(E) = N_D\delta(E - E_D). \tag{4.3}$$

This expression leads to the usual donor statistics.

(ii) We have finally considered that the conduction band edge would spread down to a value $E^* = E_C - \delta$ where, equivalently to the parameter σ, δ is an increasing function of the donor density. Then, donors whose energy E is larger than E^* are considered automatically ionized while other donors with $E < E^*$ remain localized states that can only be ionized because of the thermal energy. With the above points, the full ionized donor density is finally given by

$$\begin{aligned} N_D^+ &= \int_{E^*}^{\infty} N_D(E)\,\mathrm{d}E + \int_{-\infty}^{E^*} N_D(E) f_D(E)\,\mathrm{d}E \\ &= \frac{N_D}{2}\,\mathrm{erfc}\left(\frac{E^* - E_D}{\sigma}\right) + \frac{N_D}{\sigma\sqrt{\pi}} \int_{-\infty}^{E^*} \frac{\mathrm{e}^{((E-E_D)/\sigma)^2}}{1 + g\,\mathrm{e}^{(E_F-E)/KT}}\,\mathrm{d}E \end{aligned} \tag{4.4}$$

where erfc is the complementary error function. An estimate of the dispersion parameters σ and δ may be chosen under the form

$$\sigma \cong \delta = \alpha \frac{e^2}{4\pi\varepsilon_0\varepsilon_L d} \tag{4.5}$$

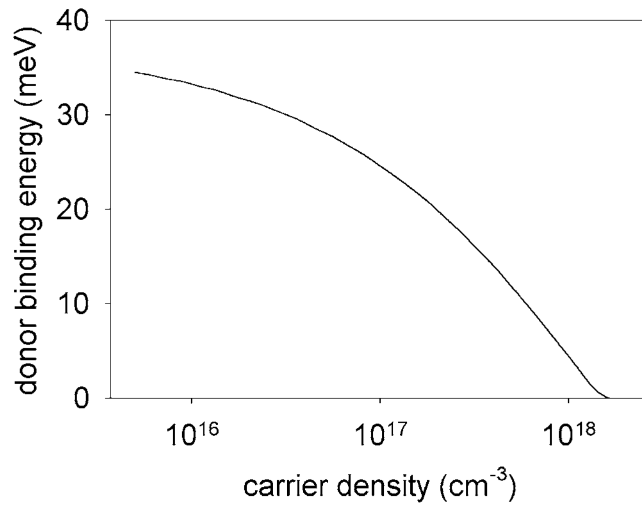

Figure 4. Impurity binding energy versus the donor density in the hydrogenic impurity model calculated with $m_{C^*} = 0.22m_0$ and $\varepsilon_L = 8.9$.

where $d \approx (N_D)^{-1/3}$ represents the mean spacing between impurities. α is a fitting parameter that depends on the donor spatial distribution, i.e. on the growth process. For low dopant densities N_D, σ and δ are then sufficiently small and the impurity density of states tends towards the $N_D\delta(E - E_D)$ Dirac function while $E^* \to E_C$: the usual statistics description. In contrast, for extremely large dopant densities, $E_D(n)$ equals zero and expression (4.5) guarantees that practically all the N_D donors are automatically ionized as expected in the case of heavily doped materials. The above expressions are only intuitively grounded. They must be considered as a way to get a continuous description of the donor statistics ranging from moderate to heavy doping.

5. Theoretical results

Using this model, we are able to simulate quantitatively the steep transition of the mobility-density plot taking realistic parameters. Figure 5 shows two theoretical curves that can fit the experimental trends presented in figure 1. The values for the high mobility regime have been intentionally chosen 20% higher in order to account for the fact that the experimental Hall mobility is slightly lower than the free carrier mobility (see for instance [5]). It appears clearly that the distance of neighbouring dislocations needs to be increased almost by a factor of 2 in order to account for a shift of the collapse by a factor of 4 between α and Ω series: typically the average equidistance of dislocations in the series α should be chosen equal to 65 nm. The compensation ratio has to be chosen slightly higher for the series α than for the better quality series Ω (0.4 and 0.3 respectively). The dislocation densities needed for the fit have been respectively taken equal to 2×10^{10} and 5×10^9 cm^{-2} in agreement with the TEM estimations [5, 8]. The location of the dislocation level under the conduction band turns out to be a sensible parameter that determines the mobility value and behaviour in the low mobility range. The better fit of the experimental results shown in figure 1 corresponds to a location at about 200 meV under the conduction band. Such a value noticeably differs from that (100 meV) found in [18] using intrinsic arguments. This may be a hint that as-grown dislocation levels do result from an extrinsic decoration of the dislocation line by some impurities or point defects.

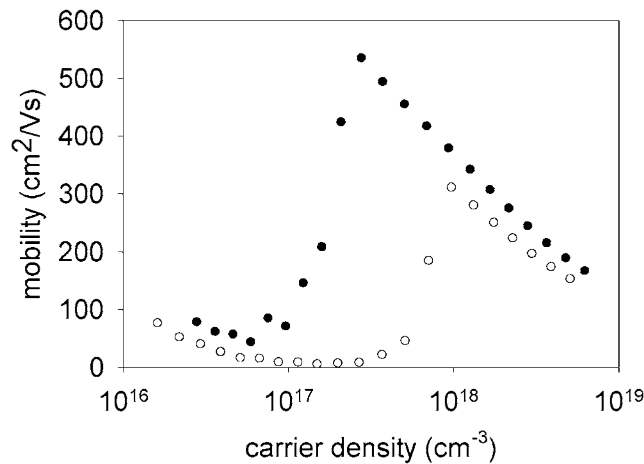

Figure 5. Modelling of the mobility versus carrier density obtained at 300 K for two different distances between neighbouring dislocations. Open circles: $d = 380$ Å and a compensation ratio equal to 0.4. Full circles: $d = 650$ Å with a compensation ratio equal to 0.3.

6. Conclusion

Inserting a comprehensive list of scattering mechanisms (ionized impurities, acoustical and optical phonons, carrier–carrier scattering) and including all the characteristics of dislocation trapping and scattering mechanisms in our low field transport simulation code, it was impossible to find any configuration leading to a good description of the experimental behaviour of the mobility versus the carrier concentration in terms of pure diffusion mechanisms. Instead, we paid attention to the dislocation substructure mainly built up of dislocation walls (sub-grain boundaries). Assuming that the dislocation density of states is responsible for some band bending around the dislocation lines, we could deduce a condition indicating when the carrier mobility is either controlled by internal electronic barriers (as long as the dielectric response of the material remains unable to separate the band bending of neighbouring dislocations) or would simply correspond to some diffusion processes associated with independent dislocations. Such a simple model fits quite well the mobility behaviour versus carrier density in columnar cells GaN samples and clearly illustrates the importance of the role of the dislocation spatial distribution (the defect 'substructure'), which, to our best knowledge, is generally neglected in similar dislocation problems. Finally, it allows us to claim that dislocations are, at least in our samples, responsible for extrinsic linear density of states localized in the mean at about 200 meV under the conduction band.

References

[1] Chin V W L, Tanley T L and Osotchan T 1994 *J. Appl. Phys.* **75** 7365–72
[2] Ridley B K 1998 *J. Appl. Phys.* **84** 4020–1
[3] Ridley B K 1998 *J. Phys.: Condens. Matter* **10** 6717–26
[4] Subhabrata Dhar and Subhasis Ghosh 1999 *J. Appl. Phys.* **86** 2668–76
[5] Bougrioua Z, Farvacque J L, Moerman I, Demeester P, Harris J J, Lee K, Van Tendeloo G, Lebedev O and Thrush E J 1999 *Phys. Status Solidi* b **216** 571–5
[6] Farvacque J L, Bougrioua Z, Moerman I, Van Tendeloo G and Lebedev O 1999 *Physica* B **273/274** 140–3
[7] van der Stricht W, Moerman I, Demeester P, Crawley J A, Thrush E J, Middelton P G, Trager-Cowan C and O'Donnell K 1995 *Proc. MRS Fall Meeting (Boston)* p 231

Bougrioua Z, Moerman I, Demeester P, Trush E J, Guyaux J-L and Garcia J-C 1999 *Proc. 8th Eur. Workshop on MOVPE (Prague)* p 61
[8] Bougrioua Z *et al* 2000 *Proc. 4th Eur. GaN Workshop (Nottingham, July) J. Cryst. Growth* at press
[9] Weimann N G, Eastman L F, Doppalapudi D, Ng H M and Moustakas T D 1998 *J. Appl. Phys.* **83** 3656–9
[10] Ng H M, Doppalapudi D, Moustakas T D, Weimann N G and Eastman L F 1998 *Appl. Phys. Lett.* **73** 821–3
[11] Albrecht J D, Ruden P P, Bellotti E and Brennan K F 1999 *MRS Internet J. Nitride Semicond. Res.* **486** vol 4S1 G6.6
[12] Look D C and Sizelove J R 1999 *Phys. Rev. Lett.* **82** 1237–40
[13] Tang H, Webb J, Bardwell J, Leathem B, Charbonneau S and Raymond S 2000 *J. Electron. Mater.* **29** 268–73
[14] Farvacque J-L 1995 *Semicond. Sci. Technol.* **18** 914–21
[15] Farvacque J-L 2000 *Phys. Rev.* B **62** 2536
[16] Seeger K 1973 *Semiconductor Physics* (Wien: Springer) p 202
[17] Elsner J, Jones R, Heggie M I, Sitch P K, Haugk M, Frauenheim Th, Oberg S and Briddon P R 1998 *Phys. Rev.* B **58** 12 571
[18] Farvacque J-L and François Ph 1999 *Physica* B **273/274** 995–8
[19] Read W T 1954 *Phil. Mag.* **45** 335
Read W T 1954 *Phil. Mag.* **45** 1119
[20] Labusch R and Schröter W 1980 *Dislocations in Solids* vol 5 (Amsterdam: North-Holland) p 129
Masut R A, Penchina C and Farvacque J-L 1982 *J. Appl. Phys.* **53** 4864
[21] Dexter D L and Seitz F 1952 *Phys. Rev.* **86** 964
Merten L 1964 *Phys. Kondens. Materie* **2** 53
Faivre G and G Saada G 1972 *Phys. Status Solidi* b **52** 127
Bougrioua Z, Ferre D and Farvacque J-L 1996 *J. Appl. Phys.* **79** 1536
[22] Shi C, Asbeck P M and Yu E T 1999 *Appl. Phys. Lett.* **74** 573–5
[23] Seto J Y W 1975 *J. Appl. Phys.* **46** 5247–54
[24] Fehrer M, Einfeldt S, Birkle U, Gollnik T and Hommel D 1998 *J. Cryst. Growth* **189/190** 763–7
[25] Salzman J, Uzan-Saguy C, Kalish R, Richter V and Mayler B 2000 *Appl. Phys. Lett.* **76** 1431–3